

Investigation of torsion, warping and distortion of large container ships

Ivo Senjanović*, Nikola Vladimir and Marko Tomić

*Faculty of Mechanical Engineering and Naval Architecture, University of Zagreb,
1. Lučića 5, 10000 Zagreb, Croatia*

(Received January 26, 2011, Accepted March 11, 2011)

Abstract. Large deck openings of ultra large container ships reduce their torsional stiffness considerably and hydroelastic analysis for reliable structural design becomes an imperative. In the early design stage the beam model coupled with 3D hydrodynamic model is a rational choice. The modal superposition method is ordinary used for solving this complex problem. The advanced thin-walled girder theory, with shear influence on both bending and torsion, is applied for calculation of dry natural modes. It is shown that relatively short engine room structure of large container ships behaves as the open hold structure with increased torsional stiffness due to deck effect. Warping discontinuity at the joint of the closed and open segments is compensated by induced distortion. The effective torsional stiffness parameters based on an energy balance approach are determined. Estimation of distortion of transverse bulkheads, as a result of torsion and warping, is given. The procedure is illustrated in the case of a ship-like pontoon and checked by 3D FEM analysis. The obtained results encourage incorporation of the modified beam model of the short engine room structure in general beam model of ship hull for the need of hydroelastic analysis, where only the first few natural modes are of interest.

Keywords: container ship; engine room; torsion; warping; distortion; analytics; FEM.

1. Introduction

In spite of the fact that ship hydroelastic behaviour is known for many years (Bishop and Price 1979), nowadays it is becoming more actual problem related to large container ships (Payer 2001, RINA 2006). These ships are especially sensitive to torsion due to large deck openings and conventional strength analysis based on the rigid body wave load is not reliable enough (Valsgård *et al.* 1995, Shi *et al.* 2005). In the early design stage, when ship structure is not yet determined in details, use of the beam model of hull girder for coupling with 3D hydrodynamic model, is preferable (Malenica *et al.* 2007).

The modal superposition method is usually used for hydroelastic analysis and the beam structural model has to describe the ship hull dry natural modes successfully. The natural modes are input data for determining modal structural stiffness, restoring stiffness, hydrodynamic coefficients and wave load (Tomašević 2007).

The transverse bulkheads in large container ships are quite robust in order to increase torsional stiffness and reduce distortion of cross-section. Height of their girders and stools is equal to the

*Corresponding author, Professor, E-mail: ivo.senjanovic@fsb.hr

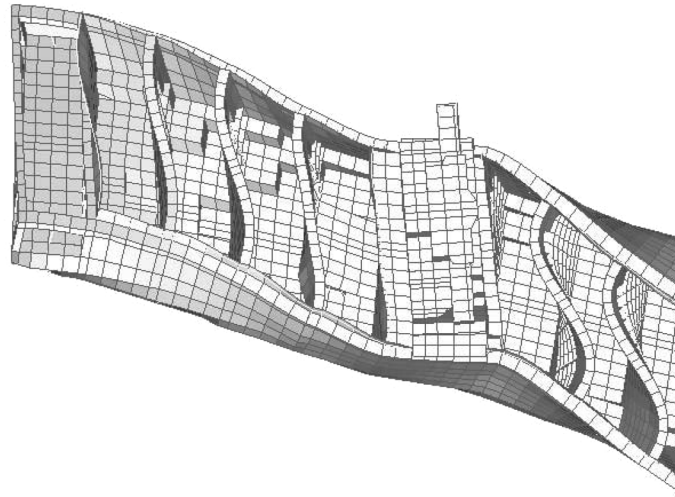


Fig. 1 Bird's eye view of the 7800 TEU container ship aftbody, the 2nd natural mode

frame spacing, i.e., ca. 2 m. Due to larger number of bulkheads their influence can be taken into account by increasing value of St. Venant torsional stiffness proportionally to the bulkhead strain energy and of the corresponding open hull portion strain energy (Senjanović *et al.* 2008).

Stiffness of the short engine room structure is reduced, that makes another problem related to large container ships. Its complex deformation is illustrated in the case of a 7800 TEU container ship, Fig. 1. The deck in-plane shear deformation is dominant, as well as bending of the stool on the top of the transverse bulkheads. The engine room front and aft bulkhead are less skewed than the hold bulkheads. Warping of the transom is very small, that is an important fact when specifying boundary conditions for torsional vibrations of beam model.

Main problem related to beam model of container ship is to satisfy warping compatibility at the joint of the closed engine room structure with the open hold cross-section. A sophisticate solution, assuming that the cross-section discontinuity is compensated with the induced horizontal bending, is presented in (Pedersen 1983, 1985). That solution is realistic for joint of long open and closed segments of ship hull. However, in the considered case of the short engine room structure, 3D FEM analysis shows that discontinuity at joint with open holds is compensated with distortion of cross-sections.

This paper aims to determine the effective values of stiffness parameters of short engine room structure in the beam model, based on energy approach. Due to small aspect ratio, length/breadth, the engine room structure behaves as the open hold structure with increased torsional stiffness. Therefore, torsionally induced horizontal bending is small and can be neglected, which makes the determination of the effective values of torsional stiffness parameters much easier (Senjanović *et al.* 2010). In addition, distortion of the engine room transverse bulkheads is considered based on known torsional and warping response. The basic formulae of thin-walled girder theory are used and the procedure is verified by a 3D FEM analysis of ship-like pontoon.

2. Basic formulae for beam torsion

The torsional thin-walled girder theory is based on the assumption that the structure behaves as a

membrane and that there is no distortion of cross-section (Vlasov 1961, Haslum and Tonnesen 1972, Steneroth and Ulfvarson 1976). In the advanced torsional beam theory, shear influence on torsion is taken into account in a similar manner to that in the flexural beam theory (Pavazza 2005). Hence, twist angle consists of a pure twist angle and a shear contribution

$$\psi = \psi_t + \psi_s \quad (1)$$

where the latter depends on the former

$$\psi_s = -\frac{EI_w d^2 \psi_t}{GI_s dx^2} \quad (2)$$

E and G are Young's modulus and shear modulus, respectively, and I_w and I_s are the warping modulus and the shear moment of inertia of cross-section, respectively (Senjanović *et al.* 2009).

The sectional forces include torque T , consisted of pure torque T_t and warping contribution T_w , and bimoment B_w , as a result of the primary and secondary shear stress fields, and normal stress due to restrained warping (Senjanović *et al.* 2009)

$$T = T_t + T_w, \quad T_t = GI_t \frac{d\psi_t}{dx} \quad (3)$$

$$T_w = GI_s \frac{d\psi_s}{dx} = -EI_w \frac{d^3 \psi_t}{dx^3} \quad (4)$$

$$B_w = EI_w \frac{d^2 \psi_t}{dx^2} \quad (5)$$

where I_t is the torsional modulus.

The governing differential equation yields from the equilibrium of the total sectional torque with the distributed external torsional load, $dT = -\mu_x dx$, Fig. 2

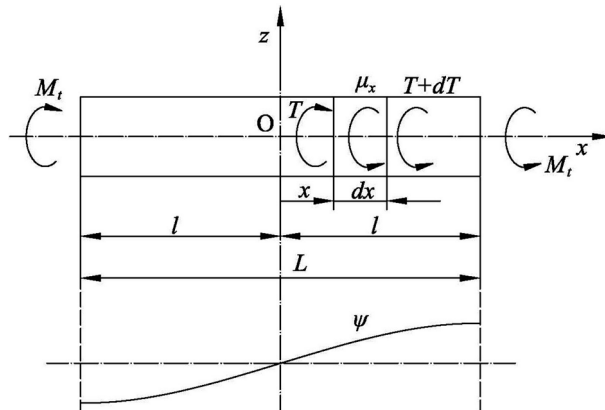


Fig. 2 Beam torsion

$$EI_w \frac{d^4 \psi_t}{dx^4} - GI_t \frac{d^2 \psi_t}{dx^2} = \mu_x \quad (6)$$

Its solution reads

$$\psi_t = A_0 + A_1 \frac{x}{l} + A_2 \operatorname{ch} \alpha x + A_3 \operatorname{sh} \alpha x + \psi_p \quad (7)$$

where

$$\alpha = \sqrt{\frac{GI_t}{EI_w}} \quad (8)$$

and ψ_p is a particular solution. The total twist angle (1) takes form

$$\psi = A_0 + A_1 \frac{x}{l} + A_2 \left(1 - \frac{I_t}{I_s}\right) \operatorname{ch} \alpha x + A_3 \left(1 - \frac{I_t}{I_s}\right) \operatorname{sh} \alpha x + \psi_p - \frac{EI_w}{GI_s} \psi_p'' \quad (9)$$

Now, it is possible to determine sectional forces by Eqs. (3), (4) and (5). The axial displacement and normal stress read, respectively

$$u = w \psi_t', \quad \sigma = Ew \psi_t'' \quad (10)$$

where w is the warping function.

3. Torsional stiffness of the engine room structure

Up to now the problem is considered assuming that there is no distortion of the cross-section. Discontinuities of the hull beam due to both deck stool and wide deck strip are analysed in (Pedersen 1983, 1985). The bending and shear effects of the stool are included in the equilibrium of the bimoments as a discontinuity. The shear and normal stress distribution of a wide deck strip acting on the hull beam contributes to the generalized hull sectional forces, i.e., bimoment, transverse shear force, torsional moment and horizontal bending moment. Hence, a pure torsional load induces horizontal bending, and the distributed sectional forces are incorporated into the mathematical model through the governing equilibrium differential equation.

In the case of a short engine room, torsion induces distortion, while bending is negligible and this complex problem is solved here by the energy balance approach and by applying the concept of effective stiffness for reasons of simplicity. A closed hull segment is considered as an open one with deck influence. For this purpose the deck strain energy is determined as follows.

The upper deck is exposed to large deformation, while the double bottom in-plane deformation is quite small, Fig. 1. The relative axial displacement of the internal upper deck boundaries, with respect to the double bottom, is a result of their warping, Fig. 3

$$U = |U_D| + |U_B| = (|w_D| + |w_B|) \psi_t' \quad (11)$$

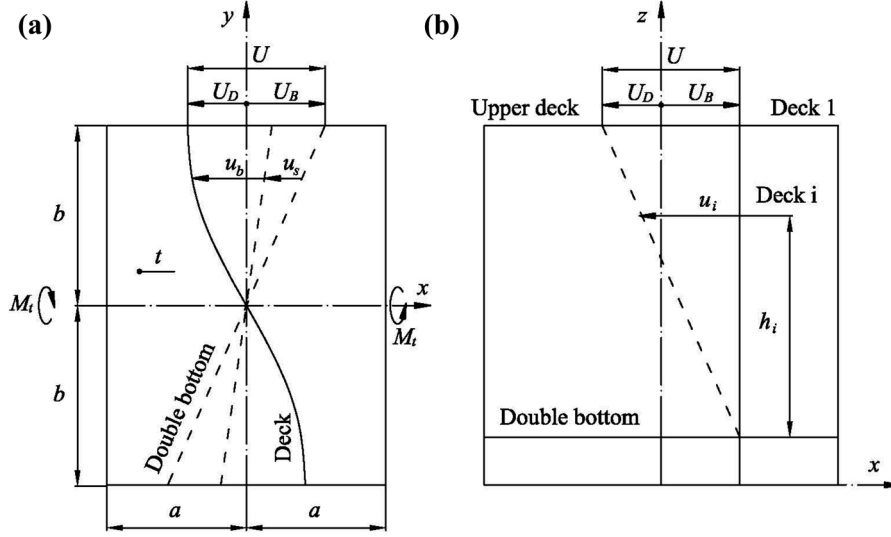


Fig. 3 Upper deck deformation and double bottom rotation, (a) bird's eye view, (b) lateral view

This causes deck in-plane deformation and the problem can be solved in an approximate analytical way by considering the deck as a beam. Its horizontal anti-symmetric deflection consists of pure bending and shear contribution, Fig. 3. The former is assumed in the form

$$u_b = \frac{y}{2b} \left[3 - \left(\frac{y}{b} \right)^2 \right] U_b \quad (12)$$

which satisfies the relevant boundary conditions: $u_b(0) = 0$ and $u_b''(0) = 0$, where U_b is the boundary bending deflection. Shear deflection depends on the bending deflection (12)

$$u_s = -\frac{EI}{GA} \frac{d^2 u_b}{dy^2} = 2(1+\nu) \left(\frac{a}{b} \right)^2 \frac{y}{b} U_b \quad (13)$$

where the internal deck cross-section area, $A = 2at_1$, its moment of inertia, $I = \frac{2}{3}a^3 t_1$, and the relation $E = 2(1+\nu)G$, are taken into account, Fig. 3. Total deflection is obtained by summing up Eqs. (12) and (13), i.e., $u = u_b + u_s$. The relation between the total boundary deflection and the bending boundary deflection reads

$$U = \left[1 + 2(1+\nu) \left(\frac{a}{b} \right)^2 \right] U_b \quad (14)$$

The total internal deck strain energy consists of the bending and shear contributions

$$E_1 = \frac{1}{2} EI \int_{-b}^b \left(\frac{d^2 u_b}{dy^2} \right)^2 dy + \frac{1}{2} GA \int_{-b}^b \left(\frac{du_s}{dy} \right)^2 dy \quad (15)$$

By substituting Eqs. (12) and (13) into (15), one finds

$$E_1 = 4(1+\nu)Gt_1\left(\frac{a}{b}\right)^3\left[1+2(1+\nu)\left(\frac{a}{b}\right)^2\right]U_b^2 \quad (16)$$

Finally, by taking into account Eqs. (11) and (14), yields

$$E_1 = \frac{4(1+\nu)Gt_1\left(\frac{a}{b}\right)^3}{1+2(1+\nu)\left(\frac{a}{b}\right)^2}(|w_D|+|w_B|)^2\psi_t'^2 \quad (17)$$

On the other hand, the total energy of the closed hull segment can be obtained by summing up the warping and twisting strain energy of the open segment, marked as (\circ), the deck strain energy and work of distributed torque, i.e.,

$$E_{tot}^* = E_w^\circ + E_t^\circ + E_1 - E_\mu \quad (18)$$

where

$$E_w^\circ = \frac{1}{2} \int_{-a}^a B_w^\circ \psi_t'' dx \quad (19)$$

$$E_t^\circ = \frac{1}{2} \int_{-a}^a T_t^\circ \psi_t' dx \quad (20)$$

$$E_\mu = \int_{-a}^a \mu_x \psi dx \quad (21)$$

Strain energy of the transverse bulkheads is not taken into account since it is quite small comparing to above ones. Within a short span $2a$, the constant value of ψ_t' (as for the deck) can be assumed, so that Eq. (20), by inserting T_t° from Eq. (3), leads to

$$E_t^\circ = GI_t^\circ a \psi_t'^2 \quad (22)$$

Furthermore, E_t° and E_1 in (18) can be contracted in one term since both depend on $\psi_t'^2$

$$E_t^\circ + E_1 = Ga\tilde{I}_t \psi_t'^2 \quad (23)$$

where

$$\tilde{I}_t = (1+C)I_t^\circ, \quad C = \frac{E_1}{E_t^\circ} \quad (24 \text{ (a), (b)})$$

\tilde{I}_t is the effective torsional modulus which includes both open cross-section and deck effects.

The engine room structure is designed in such a way that the hold double skin continuity is ensured and necessary decks are inserted between the double skins. Eq. (17) for the strain energy is

derived for the first (main) deck, and for the others it can be assumed that their strain energy is proportional to the deck plating volume, V , and linearly increasing deformation with the deck distance from the inner bottom, h , Fig. 3, since the double bottom is much stiffer than the decks. In this way, the coefficient C , Eq. (24(b)), by employing (17) and (22), reads

$$C = \frac{\sum E_i}{E_t^{\circ}} = \frac{4(1+\nu)t_1 \left(\frac{a}{b}\right)^3 (|w_D| + |w_B|)^2 k}{\left[1 + 2(1+\nu)\left(\frac{a}{b}\right)^2\right] I_t^{\circ} a} \quad (25)$$

where

$$k = \sum \frac{V_i}{V_1} \left(\frac{h_i}{h_1}\right)^2. \quad (26)$$

The general expressions for a thin-walled girder, Section 2, are still applicable for a closed segment but with the effective stiffness moduli \tilde{I}_t , \tilde{I}_w and \tilde{I}_s instead of the actual ones I_t^* , I_w^* and I_s^* . The above theory is elaborated in details in (Senjanović *et al.* 2010).

4. Distortion of segmented pontoon

Open and closed cross-section segments are connected at the transverse bulkhead, which is subjected to distortion due to different shear flows on its front and back side, induced by the torque M_t , Fig. 4. Shear flow of the open cross-section, s° , is parabolic, while that of the closed cross-section, s^* , is uniform. The resulting side forces are $S_S = S_S^{\circ} - S_S^*$, and the deck and bottom forces read $S_D = S_D^*$ and $S_B = S_B^*$, since $S_D^{\circ} = 0$ for open section and $S_B^{\circ} = 0$ due to self equilibrium for given bottom flow s° , Fig. 4. The above shear forces satisfy the static equilibrium conditions. The internal stress equilibrium leads to distortion of transverse bulkhead, δ .

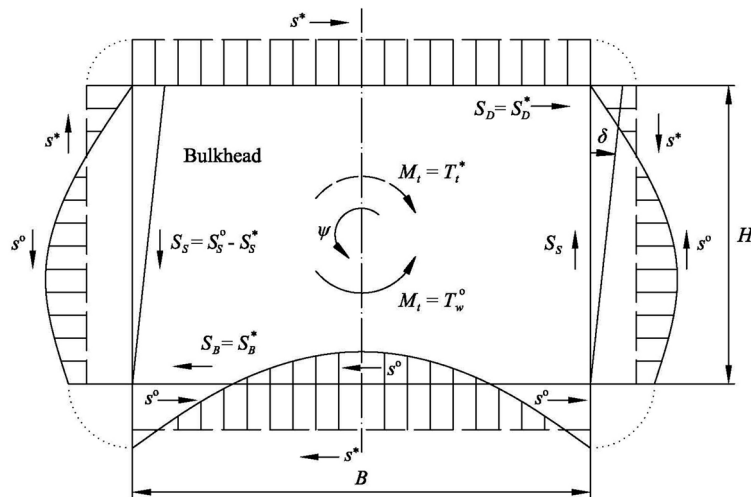


Fig. 4 Bulkhead shear forces at joint of open and closed cross-section segments

Shear flows shown in Fig. 4 are realistic for long open and closed pontoon segments. However, in the case of short closed segment, as engine room structure, the deck stiffness is reduced and its shear flow is expected to be considerably reduced, Fig. 5. As a result the remained part of cross-section behaves similarly to open one. Difference of the shear flows, $s^\circ - s^*$, is quite small but still causes bulkhead distortion, δ , which can be estimated in the following way.

Tendency of deck and double bottom of engine room structure subjected to torsion is rotation around vertical axis in opposite directions due to warping of cross-sections, Fig. 6. The total

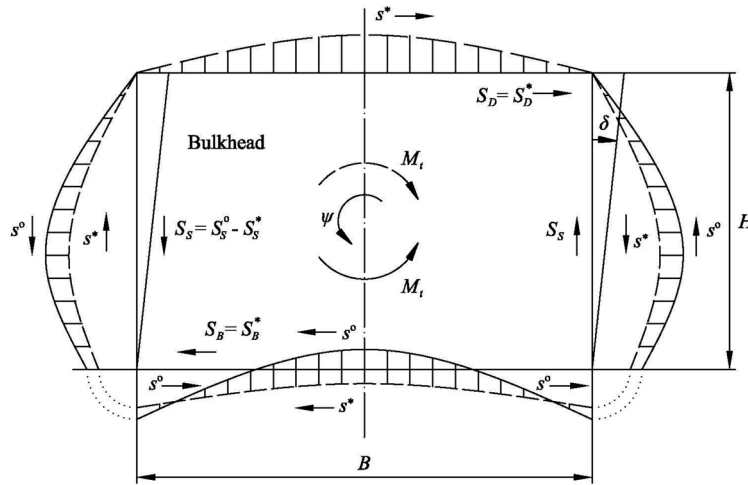


Fig. 5 Shear forces at joint of long open and short closed cross-section segments (qualitative presentation)

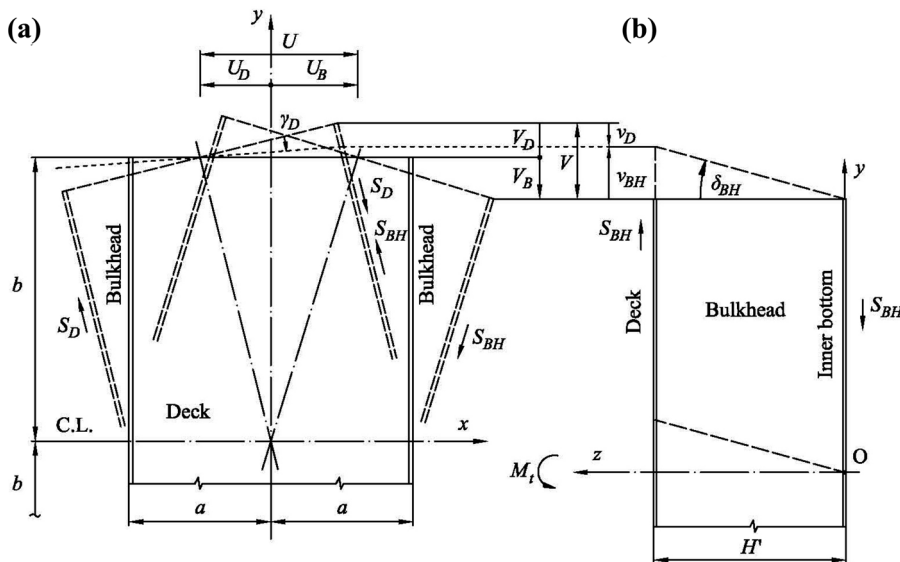


Fig. 6 Deck and bulkhead displacements and in-plane deformations, (a) bird's eye view on the deck, (b) axial view on the transverse bulkhead.

transverse gap between the deck corner and the undeformed bulkhead top, i.e., inner bottom, yields, Fig. 6

$$V = V_D + V_B = \frac{a}{b}U \quad (27)$$

where relative axial deck displacement, due to both bending and shear, with respect to double bottom, U , is given by Eq. (11). Gap V is cancelled by the deck corner transverse displacement v_D and the bulkhead top displacement v_{BH} in opposite directions, as a result of equilibrated internal shear forces S_D and S_{BH} , Fig. 6. The shear forces depend on shear deformations $\gamma_D = v_D/a$ and $\delta_{BH} = v_{BH}/H'$, respectively, where δ_{BH} is distortional angle, Fig. 6. Thus, one can write for the deck shear force

$$S_D = 2Gt_1k\frac{b}{a}v_D \quad (28)$$

where t_1 is the upper deck thickness, while k takes contribution of all decks to the resulting deck force S_D into account. It is obtained by assuming proportional increase of deck shear deformation with deck distance from the inner bottom, and moment equilibrium of shear forced S_i and S_D . That gives the same definition of k as that estimated by energy balance, Eq. (26).

In the similar way, the bulkhead shear force reads

$$S_{BH} = 2Gt_{BH}\frac{b}{H'}v_{BH} \quad (29)$$

The force equilibrium leads to the ratio of the deck and bulkhead transverse displacements

$$\frac{v_D}{v_{BH}} = \frac{t_{BH}a}{t_1kH'} \quad (30)$$

which is reciprocal to their stiffnesses. On the other hand, $v_D + v_{BH} = V$ and by taking Eqs. (11), (27) and (30) into account, one obtains

$$\delta_{BH} = \frac{v_{BH}}{H'} = \frac{(|w_D| + |w_B|)\psi'_t}{b\left(\frac{H'}{a} + \frac{t_{BH}}{t_1k}\right)} \quad (31)$$

If the bulkhead thickness increases, t_{BH} , the distortion angle decreases, and vice versa.

Distribution of the distortion angle δ within the engine room is almost linear. Along the open hold it causes horizontal bending of the upper deck boxes as beams on elastic supports, Fig. 7, (Den Hartog 1952). The support stiffness, k_e , is determined as the ratio of the imposed deck load, q , and the responded displacement, v , Fig. 8. Since the open hold is quite long, l_0 , mutual boundary influence is negligible, and therefore only the decreasing terms of homogenous solution for beam on elastic support can be used. By satisfying the relevant boundary conditions, the beam deflection in the local coordinate system, Fig. 7, reads

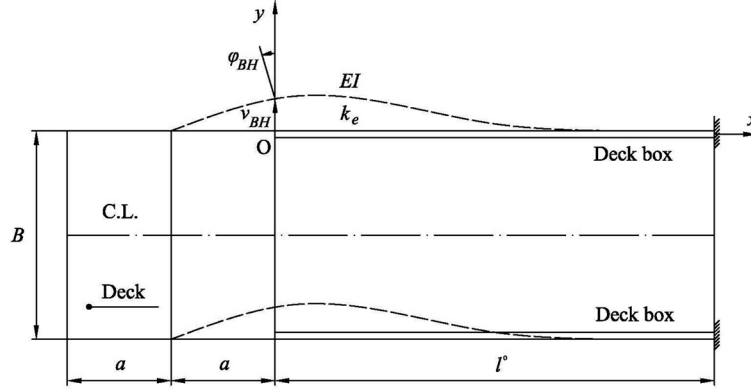


Fig. 7 Deck boxes as beams on elastic supports

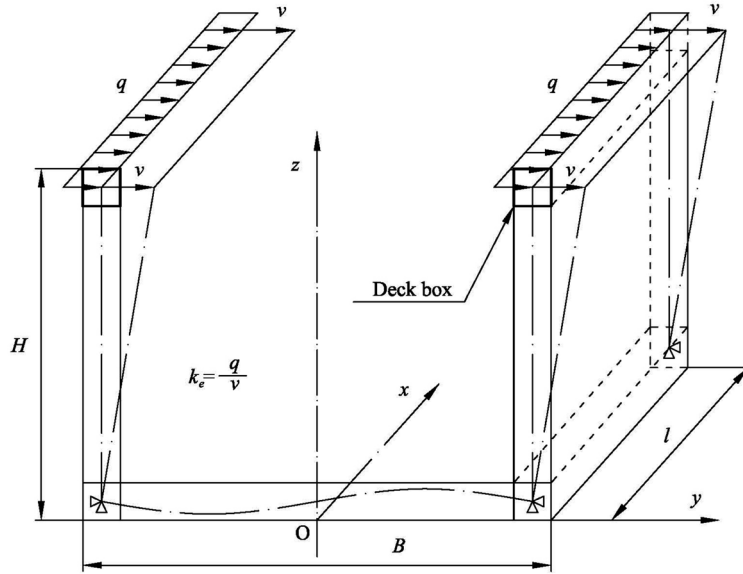


Fig. 8 Definition of deck box support stiffness

$$v = e^{-\vartheta x} \left[v_{BH} \cos \vartheta x + \left(v_{BH} + \frac{\varphi_{BH}}{\vartheta} \right) \sin \vartheta x \right] \quad (32)$$

where

$$\vartheta = \sqrt[4]{\frac{k_e}{4EI}} \quad (33)$$

EI is the beam bending stiffness, $\varphi_{BH} = v_{BH}/a$ while v_{BH} is founded from Eq. (31). Finally, function of distortion angle yields $\delta = v/H'$.

Based on the known deflection of the deck box, v , it is possible to determine its bending moment, $M = -EIv''$, and stress, $\sigma = My/I$, where y is distance of a considered point on the box cross-section from the neutral line. By employing (32) one obtains

$$\sigma_b = y \sqrt{\frac{Ek_e}{I}} e^{-\vartheta x} \left[\left(v_{BH} + \frac{\varphi_{BH}}{\vartheta} \right) \cos \vartheta x - v_{BH} \sin \vartheta x \right] \quad (34)$$

The complete stress consists of the membrane part due to restrained warping, Eq. (10), and the above bending stress, Eq. (34).

5. Torsion of a segmented girder

Let us consider a girder consisted of three segments, Fig. 9. The end segments are open and the middle one is closed, so that the girder is symmetric with respect to the z axis. Each segment is specified in its local coordinate system. The properties of the middle and end segments are designated by (*) and (°), respectively. The relevant expressions for displacements and sectional forces are specified in Section 2. The symbols A_i and B_i are used for the integration constants of the closed and open segments. The girder is loaded with torque M_t at the ends, while $\mu_x = 0$. The ends are fixed against warping.

The boundary and compatibility conditions in the considered case, yield

$$\begin{aligned} \psi^*(a) &= \psi^\circ(0), \psi_t^*(a) = \psi_t^\circ(0) \\ T^*(a) &= T^\circ(0), B_w^*(a) = B_w^\circ(0) \\ u^\circ(l^\circ) &= 0, T^\circ(l^\circ) = M_t \end{aligned} \quad (35)$$

By substituting relevant formulae for the forces and displacements from Section 2 into (35) the system of algebraic equations is formulated and its analytical solution reads

$$A_1 = \frac{M_t a}{\tilde{G}I_t}, B_1 = \frac{M_t l^\circ}{GI_t^\circ}, A_3 = \frac{D_{A3}}{D}, B_2 = \frac{D_{B2}}{D}, B_3 = \frac{D_{B3}}{D} \quad (36)$$

where

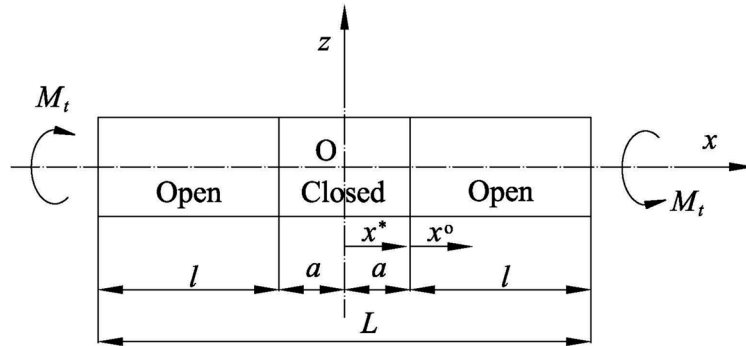


Fig. 9 Torsion of segmented girder

$$\begin{aligned}
D_{A3} &= \frac{M_t}{G} \left[\left(1 - \frac{\overset{\circ}{I}_t}{I_t}\right) \text{ch} \beta l^\circ - 1 \right] \\
D_{B2} &= -\frac{M_t}{G} \text{sh} \alpha a \left[\left(1 - \frac{\tilde{I}_t}{I_t}\right) \text{ch} \beta l^\circ + \frac{\tilde{I}_t}{I_t} \right] \\
D_{B3} &= \frac{M_t}{G} \left[\left(1 - \frac{\tilde{I}_t}{I_t}\right) \text{sh} \alpha a \text{sh} \beta l^\circ + \frac{\alpha}{\beta} \text{ch} \alpha a \right] \\
D &= \overset{\circ}{I}_t \alpha \text{ch} \alpha a \text{ch} \beta l^\circ + \tilde{I}_t \beta \text{sh} \alpha a \text{sh} \beta l^\circ
\end{aligned} \tag{37}$$

Value of constants A_0 , A_2 and B_0 is zero.

6. Geometric properties of a ship-like pontoon

A 7800 TEU Container Vessel of the following main particulars is considered:

Length overall	$L_{oa} = 334$ m
Length between perpendiculars	$L_{pp} = 319$ m
Breadth	$B = 42.8$ m
Depth	$H = 24.6$ m
Draught	$T = 14.5$ m
Displacement	$\Delta = 135530$ t.

The material properties are the following:

Young's modulus	$E = 2.06 \cdot 10^8$ kN/m ²
Shear modulus	$G = 0.7923 \cdot 10^8$ kN/m ²
Poisson's ratio	$\nu = 0.3$.

The ship lateral plan and midship section are shown in (Senjanović *et al.* 2008). The engine room is located ca. 0.2 L from the aft perpendicular, where the cross-section is reduced. However, in this numerical investigation, the engine room is extended to the full midship section so that a prismatic ship-like pontoon can be created and analysed.

The geometrical properties of the open and closed ship cross-section are determined by the program STIFF (1990) based on the strip theory of thin-walled girders (Senjanović and Fan 1992, 1993), Table 1. It is evident that the cross-section area of the closed section is 50% larger than that of the open section. The torsional modulus of the closed section is much higher than that of the open section. The shear centre of the closed section is in the middle of the cross-section, while that of the open section is below the keel.

The warping function of the open cross-section, w , is shown in (Senjanović *et al.* 2009). The relative axial displacement of the inside point of the upper deck and bilge, at the level of the inner bottom, as the representative quantities, reads $w_D = -221$ m² and $w_B = 267$ m², respectively. The relative moment of inertia of the decks volume k , Eq. (26), is calculated in Table 2.

Table 1 Geometrical properties of ship cross-sections

Quantity	Symbol, unit	Open section (°)	Closed section (*)
Cross-section area	A , m ²	6.394	10.200
Horizontal shear area	A_{sh} , m ²	1.015	2.959
Vertical shear area	A_{sv} , m ²	1.314	2.094
Vertical position of neutral line	z_{NL} , m	11.66	13.96
Vertical position of shear centre	z_{SC} , m	-13.50	9.60
Horizontal moment of inertia	I_{bh} , m ⁴	1899	2331
Vertical moment of inertia	I_{bv} , m ⁴	676	889
Torsional modulus	I_t , m ⁴	14.45	939.5
Warping modulus	I_w , m ⁶	171400	24010
Shear moment of inertia	I_s , m ⁴	710.5	173.6

Table 2 Relative moment of inertia of deck structure volume

Item i	Substructure	V_i (m ³)	h_i (m)	$\frac{V_i (h_i)^2}{V_1 (h_1)^2}$
1	Upper deck	12.738	22.6	1
2	Deck 2	14.038	18.234	0.7174
3	Deck 3	8.955	10.422	0.1495
4	Deck 4	6.434	5.214	0.0269

$$k = 1.894$$

7. Pontoon torsion and distortion

Torsion of the segmented pontoon of the total length of $L = 300$ m is analysed according to the theory presented in the previous Sections. Warping at the boundaries is restrained according to Fig. 1. Torsional moment $M_t = 40570$ kNm is imposed on the pontoon ends. The following values of the basic parameters are used: $a = 10.1$ m, $b = 19.17$ m, $t_1 = 0.01645$ m, $w_D = -221$ m², $w_B = 267$ m², $I_t = 14.45$ m⁴, Table 1, $k = 1.894$, Table 2. As a result $C = 22.42$, Eq. (25), and accordingly $\tilde{I}_t = 338.4$ m⁴, Eq. (24(a)), are obtained. Since $\tilde{I}_t = 0.36I_t^*$, effect of the short engine room structure on its torsional stiffness is obvious.

The obtained pontoon deformation functions ψ and ψ'_t are shown in Fig. 10. Distribution of distortion angle, δ , is also included in Fig. 10. It is determined by employing the procedure described in Section 4 with the following input data: $\psi'_t = 5.454 \cdot 10^{-6}$ rad/m, $H' = 22.6$ m, $t_1 = 0.01645$ m, $t_{BH} = 0.01131$ m in Eq. (31); moment of inertia of deck box cross-section $I = 0.711$ m⁴, Fig. 11, stiffness of elastic support $k_e = 721$ kN/m². Value of k_e is obtained by FEM for a pontoon open segment.

8. FEM analysis

In order to verify the numerical procedure for torsional analysis by the beam model with effective

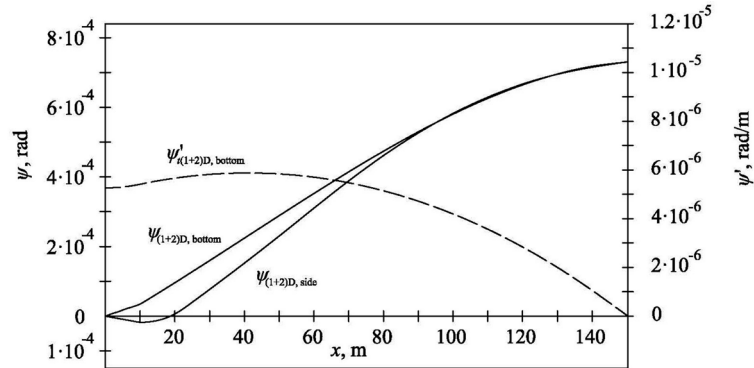


Fig. 10 Deformation functions of segmented pontoon

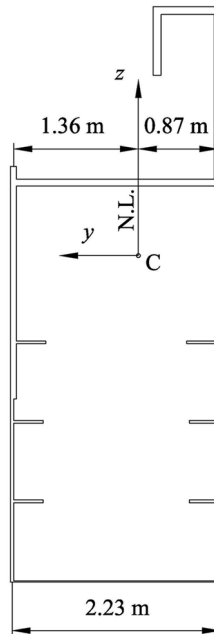


Fig. 11 Cross-section of deck box girders

stiffness parameters, designated as (1+2)D for short, 3D FEM models of the segmented pontoon are created using software SESAM (2007). The superelement technique and shell element are used. The pontoon ends are closed with transverse bulkheads. The pontoon is loaded at its ends with the vertical distributed forces in the opposite directions, generating total torque $M_t = 40570$ kNm. The midship section is fixed against transverse and vertical displacements, and the pontoon ends are constrained against axial displacements (warping).

The lateral and bird's eye views on the deformed segmented pontoon are shown in Fig. 12, and influence of the stiffer engine room structure is evident. Detailed view of this pontoon portion is presented in Fig. 13. It is apparent that the double bottom and sides rotate around the vertical axis as a “rigid body”, while the decks and transverse bulkheads are exposed to shear deformation. The



Fig. 12 Deformation of segmented pontoon, lateral and bird's eye view

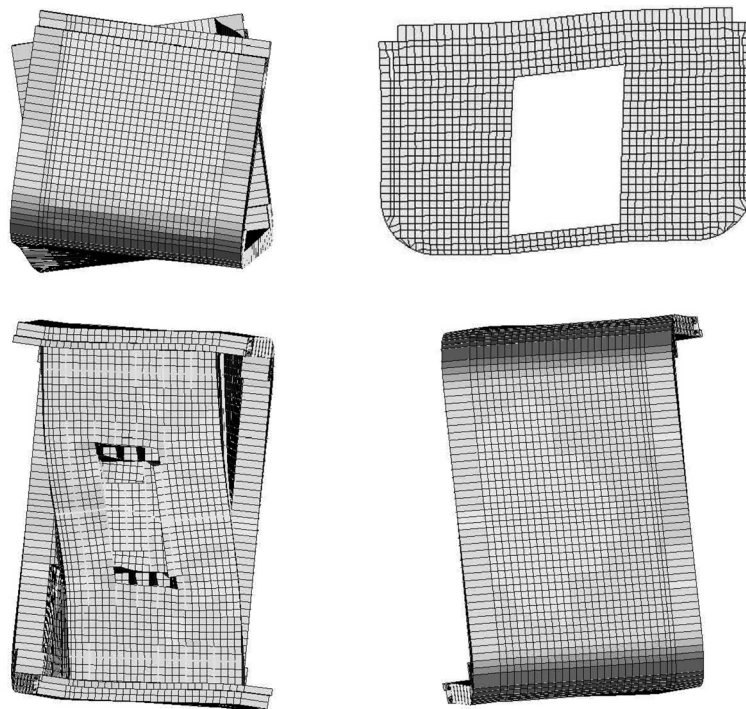


Fig. 13 Lateral, axial, bird's eye and fish views on deformed engine room superelement

shear stress distribution in the front engine room bulkhead is shown in Fig. 14. The boundary stresses, which cause distortion of cross-sections, are presented in Fig. 15. The assumed shear forces in theoretical consideration of distortion, Fig. 5, are similar to the actual boundary shear stress distribution in Fig. 15.

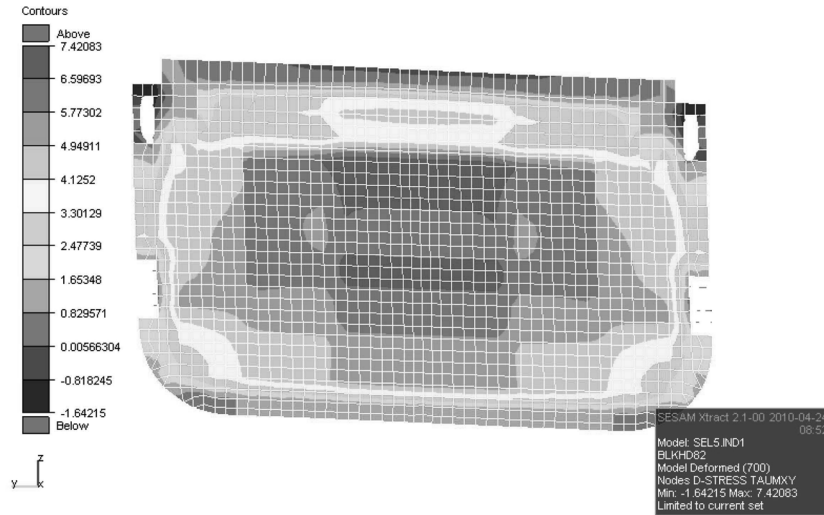


Fig. 14 Shear stresses in front engine room bulkhead

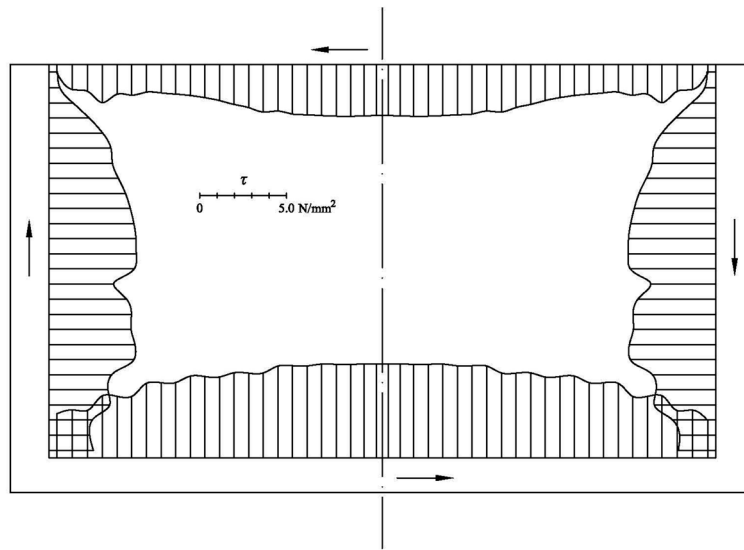


Fig. 15 Shear stresses at internal boundary of front engine room bulkhead

9. Comparative analysis

Twist angles of the analytical beam solution, $\psi_{(1+2)D}$, and that of FEM analysis, ψ_{3D} , for the pontoon bottom and side are compared in Fig. 16. As it can be noticed, there are some small discrepancies between $\psi_{(1+2)D, \text{bottom}}$ and $\psi_{3D, \text{bottom}}$, which are reduced to a negligible value at the pontoon ends

$$x = L/2: \frac{\psi_{(1+2)D, \text{bottom}}}{\psi_{3D, \text{bottom}}} = \frac{0.000733153}{0.000731985} = 1.0016$$

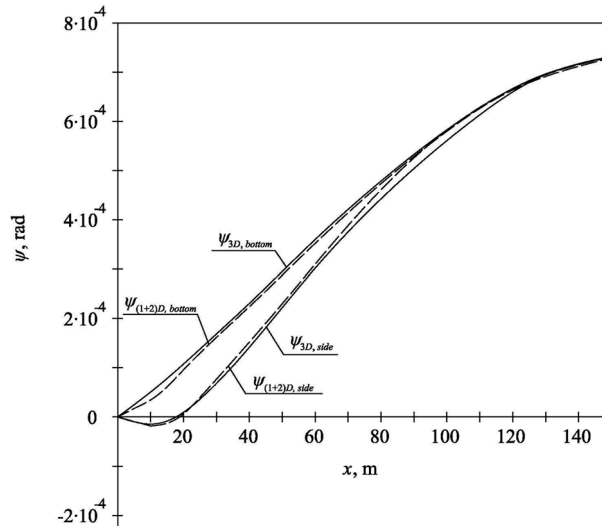


Fig. 16 Twist angles of segmented pontoon

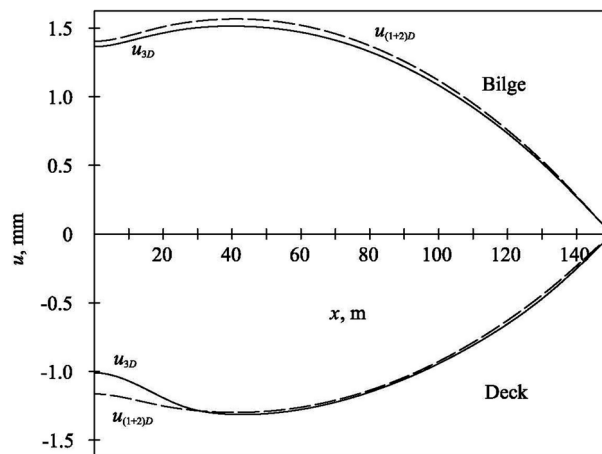


Fig. 17 Axial displacements of deck and bottom

The distortion of (1+2)D solution, $\delta_{(1+2)D} = \psi_{(1+2)D,side} - \psi_{(1+2)D,bottom}$, also follows quite well that of 3D FEM analysis, Fig. 16.

Warping of cross-section is evaluated by comparing axial displacements of the bilge and upper deck as representative points, Fig. 17. Correlation of the results obtained by the beam theory and FEM analysis is quite good from engineering point of view. There are some discrepancies between axial displacements at the deck level in the engine room area as a result of large shear deformation, Fig. 13. However, this is a local phenomenon, which can not easily be captured by the beam theory.

In order to have better insight into the structure deformation, the longitudinal distribution of the vertical position of twist centre is shown in Fig. 18. The twist centre is the corrected position of the shear centre due to shear influence on torsion, (Pavazza 2005, Senjanović *et al.* 2009). Its value is somewhat reduced in the engine room area, but it is still too far from the twist centre of the closed

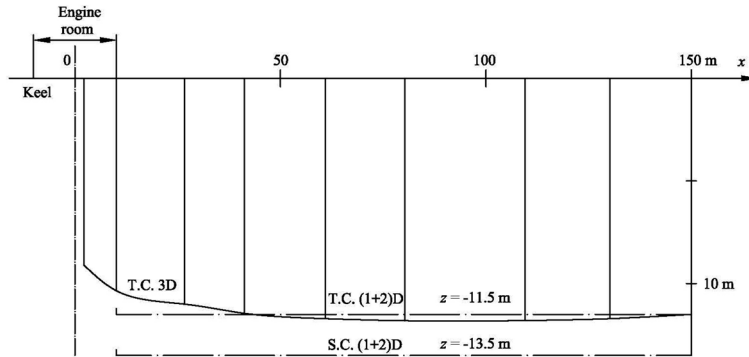


Fig. 18 Vertical position of twist centre

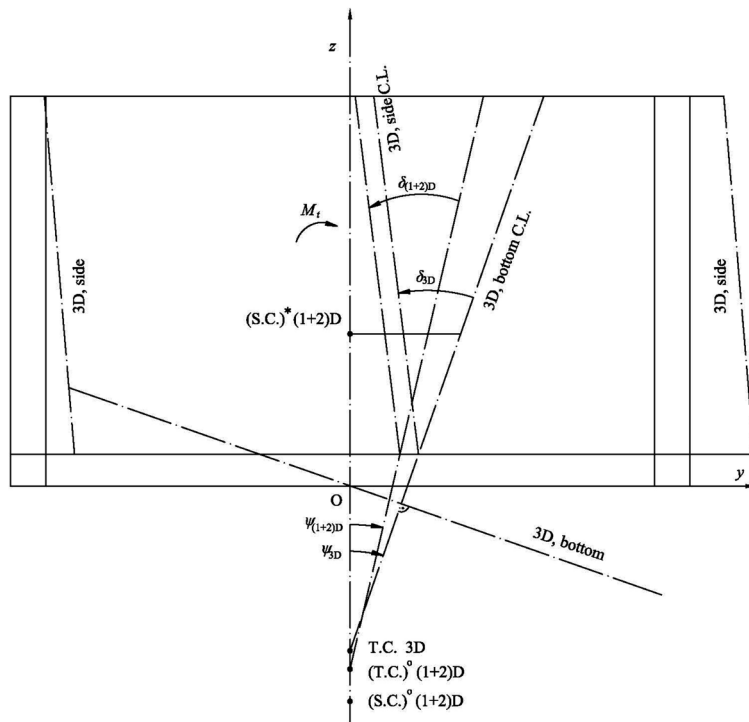


Fig. 19 Twist and distortion angles of joint cross-section of open and closed segments

segment, which would induce considerable horizontal bending. Based on the above facts, the introduced assumption of short engine room structure behaving as the open one with increased torsional stiffness is acceptable.

Deformation of the joint cross-section is shown in Fig. 19, where position of shear and twist centres for open and closed cross-sections are indicated, and compared with the position of twist centre for the real 3D structure. Also, twist angles, ψ_{3D} and $\psi_{(1+2)D}$, and distortion angle, δ , which are of the same order of magnitude, are drawn.

Longitudinal distribution of the axial normal stresses at the deck inside and outside point as well

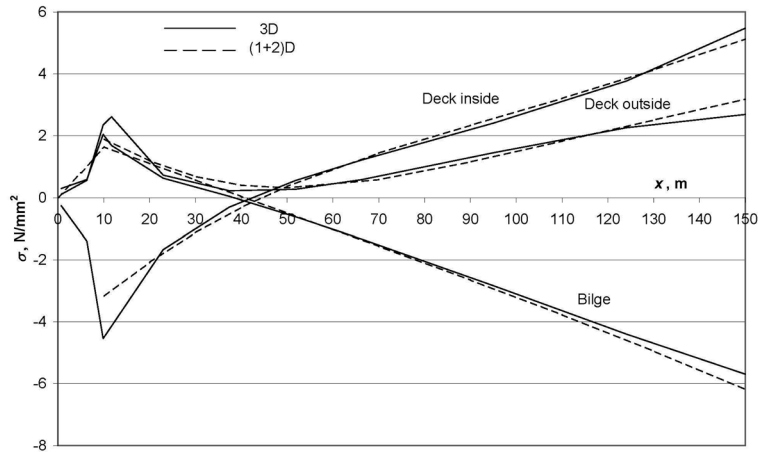


Fig. 20 Stress distributions in the upper deck and bilge (front part of pontoon, left side)

as at the bilge, determined by the (1+2)D and 3D analysis, are compared in Fig. 20. The correlation of the results is quite good from a qualitative point of view. The beam model gives somewhat smaller values of the stress concentration at the joint of the closed and open cross-section as expected. It is necessary to point out that the stress peaks determined by the 3D FEM analysis depend on the finite element mesh density.

10. Conclusions

Large container ships are quite elastic and especially sensitive to torsion due to large deck openings. Transverse bulkheads increase the hull torsional stiffness but not sufficiently. For the needs of necessary hydroelastic analysis in the early design stage use of the beam model of hull girder is preferable. A special problem is modelling of the engine room structure due to its shortness.

In this paper the effective torsional stiffness of the short engine room structure is determined by an energy approach. The most strain energy is due to the deck in-plane bending and shear deformation caused by the hull cross-section warping. The deck deformation increases proportionally with its distance from the double bottom, which mainly rotates around vertical axis as a “rigid body”. By modelling deck as a beam with shear influence on deflection, the problem is simplified.

Pontoon distortion is a result of different shear flow distributions of open and closed pontoon segments connected at the engine room bulkheads. It is estimated as the second step of calculation, based on the torsional results. Distortion is reduced by increasing bulkhead thickness.

Adoption of closed cross-section stiffness moduli and the satisfaction of compatibility conditions at the joint of the closed engine room segment with hold structure of the open cross-section presents an actual problem, related to the application of the beam model of ship hull. The offered solution for engine room structure modelling is relatively simple and its correlation with 3D FEM results in case of ship-like pontoon shows acceptable agreement of deformations and stresses. Therefore, it can be generally used for improving the beam structural model in hydroelastic analysis of relatively flexible ships such as large container vessels. Due to variable cross-section properties, the finite element method is preferable. Different beam finite elements are on disposal like (Kawai 1973), or a

sophisticated one which takes shear influence on torsion into account (Senjanović *et al.* 2009).

Acknowledgments

This investigation is carried out within the EU FP7 Project *TULCS (Tools for Ultra Large Container Ships)* and the project of Croatian Ministry of Science, Education and Sports *Load and Response of Ship Structures*. The authors would like to express their gratitude to Dr. Stipe Tomašević, University of Zagreb, for his support in generating 3D FEM models.

References

- Bishop, RED and Price, WG. (1979), *Hydroelasticity of Ships*, Cambridge University Press.
- Den Hartog, JP. (1952), *Advanced Strength of Materials*, McGraw-Hill, New York.
- Haslum, K. and Tonnessen, A. (1972), "An analysis of torsion in ship hulls", *Eur. Shipbuild.*, **5**(6), 67-89.
- Kawai, T. (1973), "The application of finite element methods to ship structures", *Comput. Struct.*, **3**(5), 1175-1194.
- Malenica, Š., Senjanović, I., Tomašević, S. and Stumpf, E. (2007), "Some aspects of hydroelastic issues in the design of ultra large container ships", *Proceedings of the 22nd International Workshop on Water Waves and Floating Bodies, IWWWFB*, Plitvice Lakes, Croatia.
- Pavazza, R. (2005), "Torsion of thin-walled beams of open cross-section with influence of shear", *Int. J. Mech. Sci.*, **47**(7), 1099-1122.
- Payer, H. (2001), "Technological and economic implications of mega-container carriers", *SNAME Transactions*, **109**, 101-120.
- Pedersen, P.T. (1983), "A beam model for the torsional-bending response of ship hulls", *RINA Transactions*, **125**, 171-182.
- Pedersen, P.T. (1985), "Torsional response of containerships", *J. Ship Res.*, **29**(3), 194-205.
- RINA (2006), *Proceedings of the International Conference on Design & Operation of Container Ships*, London.
- Senjanović, I. and Fan, Y. (1992), "A higher-order theory of thin-walled girders with application to ship structures", *Comput. Struct.*, **43**(1), 31-52.
- Senjanović, I. and Fan, Y. (1993), "A finite element formulation of ship cross-sectional stiffness parameters", *Brodogradnja*, **41**(1), 27-36.
- Senjanović, I., Tomašević, S., Rudan, S. and Senjanović, T. (2008), "Role of transverse bulkheads in hull stiffness of large container ships", *Eng. Struct.*, **30**(9), 2492-2509.
- Senjanović, I., Tomašević, S. and Vladimir, N. (2009), "An advanced theory of thin-walled girders with application to ship vibrations", *Mar. Struct.*, **22**(3), 387-437.
- Senjanović, I., Vladimir, N. and Tomić, M. (2010), "The contribution of the engine room structure to the hull stiffness of large container ships", *Int. Shipbuild. Prog.*, **57**(1-2), 65-85.
- SESAM (2007), User's Manual, Det norske Veritas, Høvik.
- Shi, B., Liu, D. and Wiernicki, C. (2005), "Dynamic loading approach for structural evaluation of ultra large container carriers", *SNAME Transactions*, **113**, 402-417.
- Steneroth, E.R. and Ulfvarson, A.Y.J. (1976), "The snaking of open ships", *Int. Shipbuild. Prog.*, **23**(257), 3-9.
- STIFF (1990), User's Manual, FAMENA, Zagreb.
- Tomašević, S. (2007), "Hydroelastic model of dynamic response of Container ships in waves", Ph.D. Thesis. University of Zagreb, Zagreb. (in Croatian)
- Valsgård, S., Svensen, T.E. and Thorkildsen, H. (1995), "A computational method for analysis of container vessels", *SNAME Transactions*, **103**, 371-393.
- Vlasov, V.Z. (1961), *Thin-walled elastic beams*, Israel Program for Scientific Translation Ltd, Jerusalem.

Nomenclature

A	– cross-section area
A_i, B_i	– integration constants
a	– one half of engine room length
B_w	– warping bimoment
C	– energy coefficient
D	– determinant
E	– Young's modulus
E_i	– strain energy
G	– shear modulus
I_s, I_t, I_w	– beam shear, torsional and warping moduli
L	– beam and pontoon length
l	– segment length
M_t	– external torque
S	– shear force
s	– shear flow
T	– torque
T_t, T_w	– twisting and warping torques
t	– plate thickness
u, v	– axial and transverse displacement
w	– warping function
x, y, z	– coordinates
$z_{S.C.}$	– ordinate of shear centre
α	– coefficient of function argument
δ	– distortion angle
μ	– distributed torque
ν	– Poisson's ratio
σ	– normal stress
ψ	– twist angle
ψ'	– twist deformation
$(\)$	– open section
$(\)^*$	– closed section
$(\)^{\sim}$	– effective value